

Band gap estimation from temperature dependent Seebeck measurement—Deviations from the $2e|S|_{\max}T_{\max}$ relation

Zachary M. Gibbs, Hyun-Sik Kim, Heng Wang, and G. Jeffrey Snyder

Citation: [Applied Physics Letters](#) **106**, 022112 (2015); doi: 10.1063/1.4905922

View online: <http://dx.doi.org/10.1063/1.4905922>

View Table of Contents: <http://scitation.aip.org/content/aip/journal/apl/106/2?ver=pdfcov>

Published by the [AIP Publishing](#)

Articles you may be interested in

[Temperature dependent band gap in PbX \(X=S, Se, Te\)](#)

Appl. Phys. Lett. **103**, 262109 (2013); 10.1063/1.4858195

[Implications of nanostructuring on the thermoelectric properties in half-Heusler alloys](#)

Appl. Phys. Lett. **101**, 133103 (2012); 10.1063/1.4754570

[Effect of antisite defects on band structure and thermoelectric performance of ZrNiSn half-Heusler alloys](#)

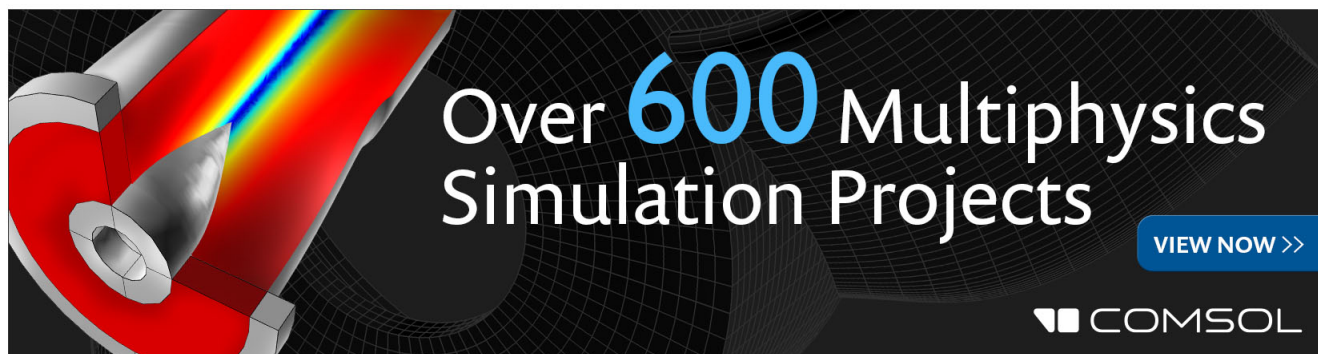
Appl. Phys. Lett. **96**, 152105 (2010); 10.1063/1.3396981

[The high temperature thermoelectric performances of Zr_{0.5}Hf_{0.5}Ni_{0.8}Pd_{0.2}Sn_{0.99}Sb_{0.01} alloy with nanophase inclusions](#)

J. Appl. Phys. **99**, 064305 (2006); 10.1063/1.2180432

[Doping-induced band edge displacements and band gap narrowing in 3C-, 4H-, 6H-SiC, and Si](#)

J. Appl. Phys. **84**, 2628 (1998); 10.1063/1.368374

The advertisement features a 3D cutaway of a mechanical part with a color gradient from red to blue, representing a simulation. The text 'Over 600 Multiphysics Simulation Projects' is prominently displayed in white and blue. A blue button with the text 'VIEW NOW >>' is located in the bottom right corner. The COMSOL logo is in the bottom right corner of the image area.

Over **600** Multiphysics Simulation Projects

[VIEW NOW >>](#)

COMSOL

Band gap estimation from temperature dependent Seebeck measurement—Deviations from the $2e|S|_{max}T_{max}$ relation

Zachary M. Gibbs,^{1(a)} Hyun-Sik Kim,^{2,3(a)} Heng Wang,² and G. Jeffrey Snyder^{2(b)}

¹Division of Chemistry and Chemical Engineering, California Institute of Technology, 1200 E. California Blvd. Pasadena, California 91125, USA

²Department of Materials Science, California Institute of Technology, 1200 E. California Blvd. Pasadena, California 91125, USA

³Materials Research Center, Samsung Advanced Institute of Technology, Samsung Electronics, Suwon 443-803, South Korea

(Received 19 November 2014; accepted 2 January 2015; published online 15 January 2015)

In characterizing thermoelectric materials, electrical and thermal transport measurements are often used to estimate electronic band structure properties such as the effective mass and band gap. The Goldsmid-Sharp band gap, $E_g = 2e|S|_{max}T_{max}$, is a tool widely employed to estimate the band gap from temperature dependent Seebeck coefficient measurements. However, significant deviations of more than a factor of two are now known to occur. We find that this is when either the majority-to-minority weighted mobility ratio (A) becomes very different from 1.0 or as the band gap (E_g) becomes significantly smaller than $10 k_B T$. For narrow gaps ($E_g \lesssim 6 k_B T$), the Maxwell-Boltzmann statistics applied by Goldsmid-Sharp break down and Fermi-Dirac statistics are required. We generate a chart that can be used to quickly estimate the expected correction to the Goldsmid-Sharp band gap depending on A and S_{max} ; however, additional errors can occur for $S < 150 \mu\text{V/K}$ due to degenerate behavior. © 2015 AIP Publishing LLC. [<http://dx.doi.org/10.1063/1.4905922>]

The maximum thermoelectric efficiency for a given material is determined by its figure of merit, $zT = \frac{S^2\sigma}{\kappa}T$, where S is the Seebeck coefficient, σ the electrical conductivity, κ the thermal conductivity, and T the temperature. In a typical plot of zT versus temperature for a good thermoelectric material (Figure 1, inset), zT will rise until reaching a peak value after which it decreases. Since the peak zT values are often the measure by which materials are compared, it is worthwhile to understand the origins of the peak and what factors can influence it. Typical degenerate thermoelectric semiconductors display thermopower (magnitude of the Seebeck coefficient, $|S|$) which rises linearly with temperature to a maximum (Figure 1(a)) followed by a decrease. Because the Seebeck coefficient is squared in the formula for zT , a maximum in the thermopower often leads to a maximum in the temperature dependent zT .

It is well known that the origin of the thermopower peak is most often related to the onset of bipolar conduction, which involves thermal excitation of both electrons and holes across the band gap. The contribution to the overall Seebeck coefficient by both the positive and negative charge carriers can be described by the conductivity weighted average

$$S = \frac{\sigma_p S_p - \sigma_n |S_n|}{\sigma_p + \sigma_n}. \quad (1)$$

Because the minority carriers are (by definition) fewer in number, they will also have higher thermopower contributions (Seebeck coefficient is inversely proportional to carrier concentration). However, at low temperatures, the population of minority carriers is small, meaning that they will not contribute much to the overall S . At higher temperatures,

though, a broadening Fermi distribution leads to an exponential increase in minority carrier conductivity resulting in a reduction (and therefore peak) in the thermopower.¹

The strength of bipolar conduction is determined by the value of the semiconductor band gap. Goldsmid and Sharp developed an analytical expression relating the band gap and the maximum thermopower, $|S|_{max}$ (defined as the magnitude of the Seebeck coefficient), and the temperature at which it occurs (T_{max}) in the bipolar regime by: $E_g = 2e|S|_{max}T_{max}$.¹ This simple method of estimating the band gap is ubiquitous in the thermoelectrics community because temperature dependent Seebeck coefficient is so commonly measured. Figure 1 shows a calculated temperature dependent Seebeck coefficient and corresponding zT (inset) for a valence (VB) and conduction band (CB) model with a band gap of 0.13 eV at various carrier concentrations. We can see that the

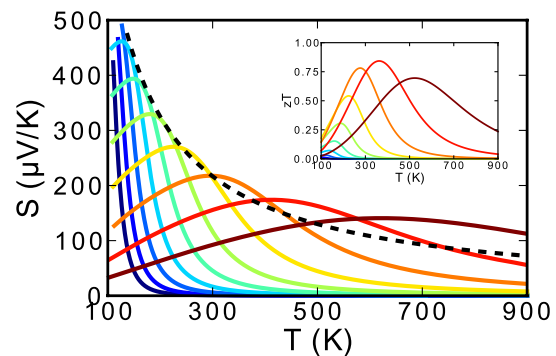


FIG. 1. Calculated temperature dependent Seebeck coefficient and zT (inset) for various defect concentrations ($N_A = p - n = 1 \times 10^{15} \text{ cm}^{-3}$ in blue to $1 \times 10^{20} \text{ cm}^{-3}$ in red) for two parabolic bands with a band gap of 0.13 eV, $m^* = 1.0 m_0$, and $\mu_0(300 \text{ K}) = 820 \text{ cm}^2/\text{Vs}$ (VB and CB). Dashed line indicates the Goldsmid-Sharp band gap: $S = E_g/2eT$. Umklapp scattering of phonons was used for the temperature dependent thermal conductivity in the zT estimate: $\kappa_L(T) = 1.7(300/T) \text{ W/m-K}$.

^{a)}Z. M. Gibbs and H.-S. Kim contributed equally to this work.

^{b)}Author to whom correspondence should be addressed: jsnyder@caltech.edu

Goldsmid-Sharp band gap formula (dashed line) accurately predicts the maximum thermopower over a wide range of carrier concentrations and temperatures.

The Goldsmid-Sharp result is useful for estimating the maximum attainable thermopower in a material. As demonstrated in Figure 1 (and S1(a)), the Goldsmid-Sharp result (dashed line) serves as a good upper bound for the thermopower at a particular temperature, regardless of extrinsic doping concentration. For example, Bi₂Te₃ has a band gap of $E_g \sim 0.13$ eV (Refs. 2 and 3) at room temperature ($T_{max} = 300$ K), yielding a maximum Seebeck coefficient near $230 \mu\text{V/K}$ —a reasonable estimate.⁴⁻⁷

While the Goldsmid-Sharp gap serves as a quick estimate of the band gap in a given material, it is important to understand where deviations might occur when using this analysis. In Goldsmid-Sharp's full equation, the weighted mobility ratio, $A = \frac{\mu_{maj} N_{v,maj} (m_{b,maj}^*)^{3/2}}{\mu_{min} N_{v,min} (m_{b,min}^*)^{3/2}} = \frac{\mu_{maj}}{\mu_{min}} \left(\frac{m_{b,maj}^*}{m_{b,min}^*} \right)^{3/2} = \frac{B_{maj}}{B_{min}}$ (where μ is the mobility, N_v is the valley degeneracy, m^* and m_b^* are the density of states and single valley effective mass, and B is the quality factor for majority and minority charge carriers), governs the relative contributions of the electron and hole bands to the electronic properties in the case of bipolar conduction. We can also consider A as the ratio of the quality factors, $B = \frac{\mu_0 m^{*3/2}}{\kappa_L}$ (where μ_0 is the non-degenerate mobility and κ_L is the lattice thermal conductivity), between the majority and minority bands, which relate directly to the maximum attainable zT (for any doping level) for a given band.⁸⁻¹² One of the primary conclusions of the Goldsmid-Sharp paper was that the $2e|S|_{max} T_{max}$ band gap was within $\sim 20\%$ of the actual value and was roughly independent of the weighted mobility ratio, but this assumed that the dimensionless band gap ($\epsilon_g = \frac{E_g}{k_B T}$)—the parameter that governs the strength of bipolar conduction—was equal to 10. For some common thermoelectric materials—Bi₂Te₃,^{13,14} PbSe,^{15,16} PbTe,^{17,18} the value of the band gap is actually 5–6 $k_B T$ at T_{max} . Recent work by Schmitt, Gibbs *et al.* shows that for ZrNiSn half-Heuslers, the Goldsmid-Sharp band gap can deviate by 50%–100% of the optical band gap value mainly due to the large majority-to-minority weighted mobility ratio ($A = 5$) and an ϵ_g much lower than the 10 used in the derivations by Goldsmid-Sharp.¹⁹ Further, because E_g is often within $\sim 6 k_B T_{max}$, Maxwell-Boltzmann statistics—applied in Goldsmid-Sharp's derivation—should be replaced with Fermi-Dirac statistics which more accurately represent semiconductor processes in narrow-gap ($\epsilon_g < 10$), heavily doped materials. We thoroughly probe the limitations of the $2e|S|_{max} T_{max}$ relation, particularly by exploring the effect of varying majority-to-minority weighted mobility ratio (A) and the dimensionless band gap (ϵ_g). We generate a chart that can be used to quickly estimate the relationship between the true and the Goldsmid-Sharp band gaps depending on A and S_{max} .

The expression for the Seebeck coefficient in a multi band (valence/conduction) can be expressed by rearranging Eq. (1)²⁰

$$S = \frac{1}{1 + \frac{\sigma_{maj}}{\sigma_{min}}} \left(S_{min} + \frac{\sigma_{maj}}{\sigma_{min}} S_{maj} \right), \quad (2)$$

where S , S_{maj} , and S_{min} are the overall, majority carrier, and minority carrier Seebeck coefficients, respectively. σ_{maj} and σ_{min}

are the majority and minority carrier conductivities, respectively. In the interest of maintaining general relationships applicable for either p or n-type materials, we chose to use the majority and minority carrier labels; in the case of a primarily p-type material, the majority carrier will be holes. While Goldsmid and Sharp proceed assuming Maxwell-Boltzmann, non-degenerate statistics— $\frac{\sigma_{maj}}{\sigma_{min}} = A \exp(\eta_{maj} - \eta_{min})$, where $A = \frac{\mu_{maj} N_{v,maj} (m_{b,maj}^*)^{3/2}}{\mu_{min} N_{v,min} (m_{b,min}^*)^{3/2}}$, we will consider the Fermi integral solution to the Boltzmann transport equation (assuming scattering by acoustic phonons and parabolic bands). In this context, the Seebeck coefficient of a specific carrier type (S_i) and electrical conductivity ratio between the majority and minority carriers can be written as a function of the dimensionless chemical potential ($\eta = \xi/k_B T$)—where ξ is the electronic chemical potential

$$S_i = \frac{k_B}{e} \left(\frac{F_2(\eta_i)}{F_1(\eta_i)} - \eta_i \right), \quad (3)$$

$$\frac{\sigma_{maj}}{\sigma_{min}} = A \frac{F_1(\eta_{maj})}{F_1(\eta_{min})}, \quad (4)$$

where A has the same definition as in the Goldsmid-Sharp formulation and represents the weighted mobility ratio and F_j represents the Fermi integral

$$F_j(\eta) = \int_0^\infty \frac{e^{\epsilon} d\epsilon}{1 + \exp(\epsilon - \eta)}. \quad (5)$$

In order to find the maximum thermopower, several methods can be used as differentiated in Table I. The derivation of the Goldsmid-Sharp band gap does not explicitly find the maximum in thermopower with temperature; rather, Goldsmid-Sharp find maxima with respect to reduced chemical potential, $dS/d\eta = 0$ which is equivalent to $dS/dT = 0$ when $d\eta/dT$ is much larger than $\frac{d(\epsilon_g)}{dT}$ as pointed out by Goldsmid and Sharp.¹ In this work, the “Fermi” method (Table I) also assumes $dS/d\eta = 0$, as in the “Goldsmid-Sharp” method, but it uses Fermi-Dirac rather than Maxwell-Boltzmann statistics. We can test the $dS/d\eta = 0$ approximation by performing a full, temperature dependent calculation of the Seebeck coefficient—the “Exact” method. This is accomplished by applying a charge counting balance, $N_A - N_D = p - n$, at various temperatures, where N_A and N_D are the number of electron acceptors and donors, respectively, and p and n are the number of holes and electrons, respectively (for simplicity, we have assumed that $A_{m^*} = \frac{m_{maj}^*}{m_{min}^*} = 1$, but we discuss the alternative in the supplementary material: Figure S4²¹). The full, temperature dependent, numerically

TABLE I. Description of the three different methods of estimating the maximum thermopower in this work.

Method name	Criterion for maximum	Statistics
Goldsmid-Sharp	$dS/d\eta = 0$	Maxwell-Boltzmann
Fermi	$dS/d\eta = 0$	Fermi
Exact	$dS/dT = 0$	Fermi

calculated results (“Exact” method) will be presented along with the simpler $dS/d\eta=0$ solutions using both Maxwell-Boltzmann (“Goldsmid-Sharp”) and Fermi-Dirac (“Fermi”) statistics.

First, in order to probe the applicability Goldsmid-Sharp’s assumption of Maxwell-Boltzmann (non-degenerate) statistics, Figure 2 (and Figure S1²¹) considers a weighted mobility ratio of $A=1$. Figure 2(a) shows the chemical potential dependent Seebeck coefficient (with $\eta=0$ being the valence band edge, $\epsilon_g=5$ being the conduction band edge). As expected, the “Goldsmid-Sharp” result overlaps well with the “Fermi” result for chemical potentials in the gap ($0 < \eta < 5$), but deviations begin for chemical potentials of about $1.5 k_B T$ from either band edge which become larger as the chemical potential becomes degenerate (chemical potential within the band, $\eta < 0$ or $\eta > \epsilon_g = 5$).

By varying ϵ_g , we can determine the maximum Seebeck coefficient using the three methods discussed in Table I—see supplementary Figure S1 for detailed results.²¹ Figure 2(b) quantifies the effectiveness of the $2e|S|_{\max}T_{\max}$ estimate for band gap at different ϵ_g for the three cases of interest: the $dS/d\eta=0$ model using both the “Fermi” and “Goldsmid-Sharp” methods, as well as the $dS/dT=0$ (or “Exact”) case. For large ϵ_g , the “Fermi” and “Goldsmid-Sharp” solutions ($dS/d\eta=0$) converge to $2e|S|_{\max}T_{\max}/E_g$ very near 1.0 (although the exact value is 3% less at $\epsilon_g=10$). However, as the band gap becomes small ($\epsilon_g \lesssim 5$), $2e|S|_{\max}T_{\max}/E_g$ increases for all three methods. The divergence for small gaps is a consequence of increasingly degenerate chemical potentials which yield the maximum thermopower. Experimentally, this would be observed for heavily doped samples that do

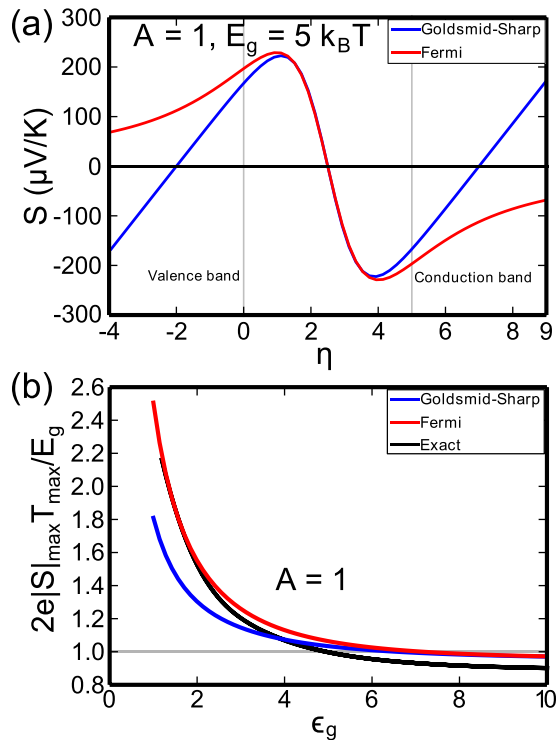


FIG. 2. Result of the “Exact,” “Fermi,” and “Goldsmid-Sharp” methods calculated assuming $\epsilon_g=5$ and $A=1$ for (a) Seebeck coefficient as a function of η , (b) the ratio of the $2e|S|_{\max}T_{\max}$ estimate to E_g as a function of the dimensionless band gap ϵ_g .

not reach a maximum thermopower until very high temperatures.

We have shown that the degree of degeneracy can result in some deviations to the Goldsmid-Sharp band gap, but the weighted mobility ratio (A) can also play a substantial role. While Bi_2Te_3 has similar majority and minority carrier weighted mobility,^{22,23} other systems such as ZrNiSn ,¹⁹ Si, Ge, and others,²⁴ are believed to have values that exceed two (5 in the case of ZrNiSn). In order to illustrate the effect of an increasing weighted mobility ratio, the η -dependent Seebeck is plotted for ZrNiSn ($\epsilon_g \sim 5$ at room temperature)¹⁹ in Figure 3(a). We see that the magnitude of the maximum Seebeck coefficient obtained for p-type ZrNiSn ($A=1/5$) is significantly lower than that for n-type ZrNiSn ($A=5$). The effect of having an A different from one is that the magnitude of the maximum Seebeck coefficient ($|S|_{\max}$) as well as the temperature where it occurs (T_{\max}) are increased for the carrier type with higher weighted mobility, while those of the lower weighted mobility carrier are decreased. So, in a

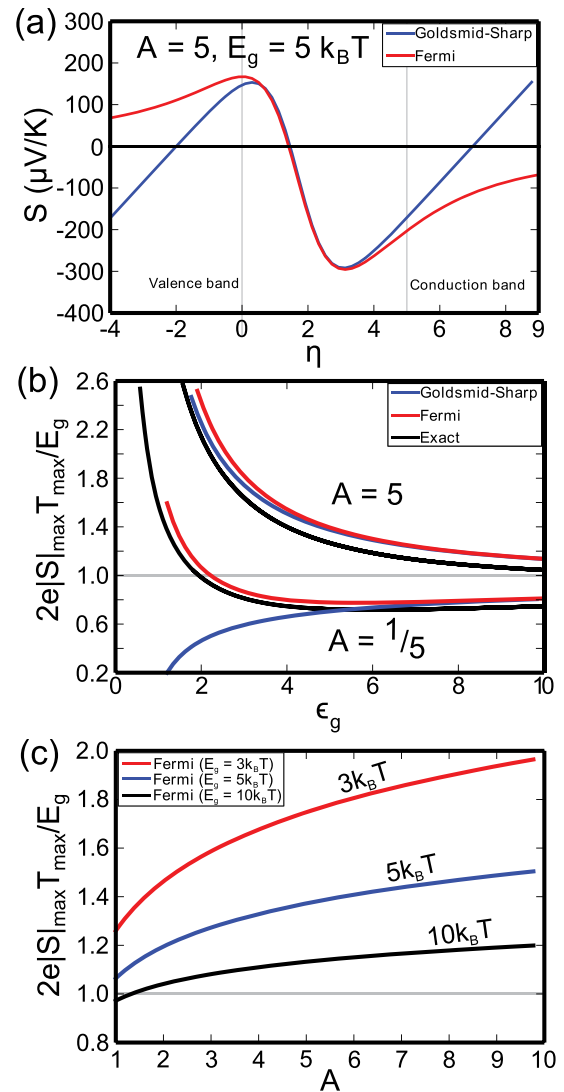


FIG. 3. Result of the “Exact,” “Fermi,” and “Goldsmid-Sharp” methods assuming $\epsilon_g=5$ and $A=5$ (weighted mobility ratio) for (a) Seebeck coefficient as a function of η , (b) the ratio of the $2e|S|_{\max}T_{\max}$ estimate to the actual model E_g as a function of ϵ_g , and (c) the same ratio with respect to the weighted mobility ratio A at different E_g values (3, 5, and $10 k_B T$ as indicated on the figure).

system like ZrNiSn, the n-type material maintains a high thermopower to much higher temperatures than might be expected from its narrow band gap (~ 0.13 eV) resulting in an impressive zT from 0.5–1.0.^{25,26} On the other hand, the p-type ZrNiSn prematurely experiences reduced thermopower due to compensating high-mobility electrons. In Figure 3(b), it is obvious that $2e|S|_{\max}T_{\max}/E_g$ is larger than 1.0 for all values of ϵ_g when $A = 5$, while it is less than 1.0 for all ϵ_g for $A = 1/5$ (except at quite low ϵ_g). Figure 3(c) shows how $2e|S|_{\max}T_{\max}/E_g$ increases with the increase in A values; larger deviations are observed as $E_g/k_B T$ becomes smaller. In comparison with Goldsmid-Sharp's conclusion that only $\sim 20\%$ deviation is observed for $A = 10$, we find that 50%–100% error in the estimated gap are predicted for ϵ_g values which are reasonable for many relevant thermoelectric materials ($\epsilon_g \sim 4$ –5). More details regarding estimations of $|S|_{\max}$ and η_{\max} are included in supplementary Figure S2.²¹

While the Goldsmid-Sharp band gap has proven to be a simple and useful estimate for the real band gap, it is not without its limitations. In this work, we have shown several cases for which this simple approximation breaks down. Figure 4 shows the deviation between the Goldsmid-Sharp band gap and the true band gap for a wide variety of these parameters. Ultimately, we observe that the magnitude of the deviation is largest for materials with large differences between the weighted mobility of electrons and holes ($A \neq 1$). From an experimental perspective, $A \neq 1$ will result in a larger value of $2e|S|_{\max}T_{\max}$ for the higher weighted mobility species, and a lower value for the one with lower weighted mobility. In the case of ZrNiSn, the more mobile electrons ($A = 5$) result in an observation of about a five-fold difference in the p-type (~ 0.05 eV) and the n-type (~ 0.25 eV) Goldsmid-Sharp band gaps.¹⁹

Figure 4 can be useful in determining either an unknown A value for a material if the true band gap is known, or it can show the expected deviations of the Goldsmid-Sharp band gap relative to the true band gap for a given A value. For instance, in the case of n-type ZrNiSn with $2e|S|_{\max}T_{\max}/$

$E_g = 2.1$ (using $E_{g,optical} = 0.13$ eV (Ref. 19)) and observed maximum Seebeck coefficient (~ 200 $\mu\text{V/K}$), Figure 4 can be used to determine $A \sim 5$. Alternatively, if the majority-to-minority carrier weighted mobility ratio (A) is known, one can (based on the magnitude of the maximum Seebeck coefficient) obtain an estimate a value for $2e|S|_{\max}T_{\max}/E_g$ from Figure 4, which can be used to estimate the true band gap (as described in the numbered list below).

- (1) Measure temperature dependent thermopower and obtain a maximum.
- (2) Calculate the Goldsmid-Sharp band gap: $E_g = 2e|S|_{\max}T_{\max}$.
- (3) If $|S|_{\max} < 150$ $\mu\text{V/K}$, be aware that the true E_g may significantly differ from $2e|S|_{\max}T_{\max}$ (see below).
- (4) For $|S|_{\max} > 150$ $\mu\text{V/K}$, estimate the majority-to-minority carrier weighted mobility ratio, A .
- (5) Find the $2e|S|_{\max}T_{\max}/E_g$ ratio (r) from Figure 4 that is consistent with that A and S_{\max} value to then calculate the corrected $E_g = 2e|S|_{\max}T_{\max}/r$.

The $S_{\max} < 150$ $\mu\text{V/K}$ describes the degenerate crossover that leads to the upward trend in Figure 4 mentioned previously for low values of S_{\max} . For degenerate, heavily doped samples (η_{\max} in the majority band), $E_g/k_B T_{\max}$ becomes a poor metric for describing the bipolar effects; rather, we believe that the thermal band gap ($\frac{E_{g,thermal}}{k_B T} = \epsilon_g + \eta$) is the relevant parameter. This effect is even more pronounced as A is decreased because the lower mobility majority carrier requires a chemical potential deep within the band (large η) to mitigate the effects of a highly mobile minority carrier (see supplementary Figures S1(b) and S2(b)²¹).

In summary, the Goldsmid-Sharp band gap ($E_g = 2e|S|_{\max}T_{\max}$) is an extremely useful tool for obtaining an estimate for a material's band gap through temperature dependent Seebeck measurements. While most researchers understand that this is not an exact estimate, it is important to understand when and why the simple relation can break down and to what extent. In this work, we show that large

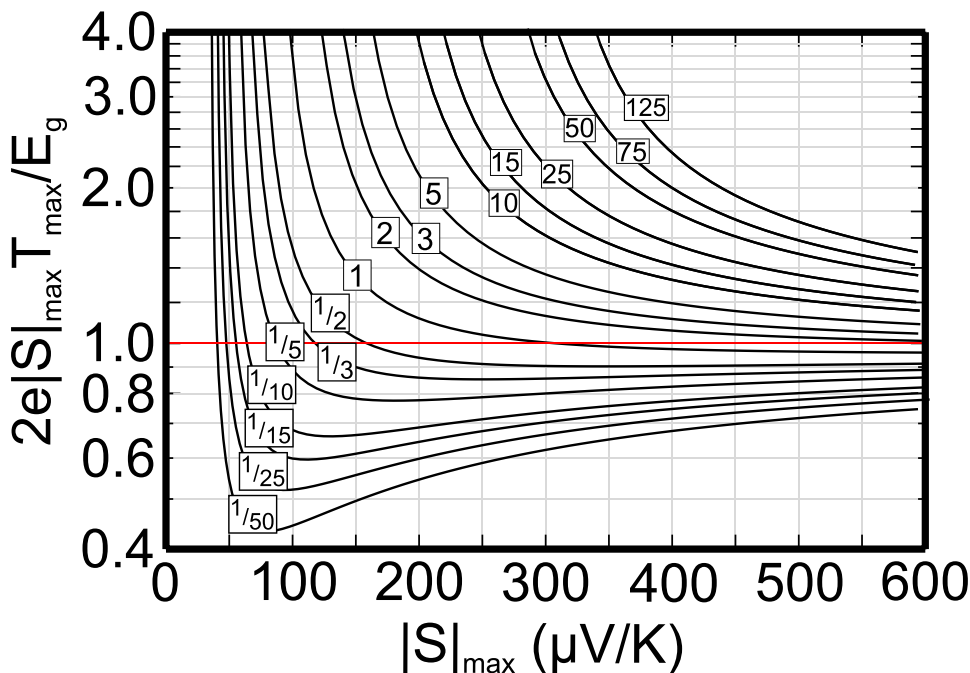


FIG. 4. The ratio of the $2e|S|_{\max}T_{\max}$ estimate to the actual model E_g as a function of thermopower for a wide variety of A and E_g values. “ A ” values are noted in a rectangular box laid on top of each black solid lines.

deviations can occur for several reasons: a breakdown of Maxwell-Boltzmann statistics (used to derive the Goldsmid-Sharp band gap) for materials with narrow gaps, or materials with very large (or small) majority-to-minority carrier weighted mobility ratio (A). Because bipolar conduction is detrimental to thermoelectric performance, results from this work using the Goldsmid-Sharp gap could be used to validate strategies for suppressing bipolar effects beyond altering band gap and doping^{14,27–29} but also by other methods (including nanostructures^{30–33}), given that both n-type and p-type samples are obtainable.

The authors would like to acknowledge funding from The Materials Project: supported by Department of Energy's Basic Energy Sciences program under Grant No. EDCBEE and DOE Contract No. DE-AC02-05CH11231.

- ¹H. J. Goldsmid and J. W. Sharp, *J. Electron. Mater.* **28**, 869–872 (1999).
- ²O. Madelung, *Semiconductors: Data Handbook* (Springer Science & Business Media, 2004).
- ³G. S. Nolas, J. Sharp, and H. J. Goldsmid, *Thermoelectrics: Basic Principles and New Materials Developments* (Springer Science & Business Media, 2001).
- ⁴M. Stordeur and W. Kühnberger, *Phys. Status Solidi B* **69**, 377–387 (1975).
- ⁵L. R. Testardi, J. N. Bierly, Jr., and F. J. Donahoe, *J. Phys. Chem. Solids* **23**, 1209–1217 (1962).
- ⁶H.-W. Jeon, H.-P. Ha, D.-B. Hyun, and J.-D. Shim, *J. Phys. Chem. Solids* **52**, 579–585 (1991).
- ⁷T. Plecháček, J. Navrátil, J. Horák, and P. Lošťák, *Philos. Mag.* **84**, 2217–2228 (2004).
- ⁸R. P. Chasmar and R. Stratton, *J. Electron. Control* **7**, 52–72 (1959).
- ⁹G. D. Mahan, *Solid State Physics* (Academic Press Inc, San Diego, 1998), Vol. 51, pp. 81–157.
- ¹⁰A. S. Glen, in *CRC Handbook of Thermoelectrics* (CRC Press, 1995).
- ¹¹Y. Pei, A. D. LaLonde, H. Wang, and G. J. Snyder, *Energy Environ. Sci.* **5**, 7963–7969 (2012).
- ¹²Y. Pei, H. Wang, and G. J. Snyder, *Adv. Mater.* **24**, 6125–6135 (2012).
- ¹³I. G. Austin, *Proc. Phys. Soc.* **72**, 545 (1958).

- ¹⁴S. Wang, G. Tan, W. Xie, G. Zheng, H. Li, J. Yang, and X. Tang, *J. Mater. Chem.* **22**, 20943–20951 (2012).
- ¹⁵H. Wang, Y. Z. Pei, A. D. LaLonde, and G. J. Snyder, *Adv. Mater.* **23**, 1366–1370 (2011).
- ¹⁶H. Wang, Y. Pei, A. D. LaLonde, and G. J. Snyder, *Proc. Natl. Acad. Sci.* **109**, 9705–9709 (2012).
- ¹⁷A. D. LaLonde, Y. Z. Pei, and G. J. Snyder, *Energy Environ. Sci.* **4**, 2090–2096 (2011).
- ¹⁸Y. Pei, A. LaLonde, S. Iwanaga, and G. J. Snyder, *Energy Environ. Sci.* **4**, 2085–2089 (2011).
- ¹⁹J. Schmitt, Z. M. Gibbs, G. J. Snyder, and C. Felser, *Mater. Horiz.* **2**, 68–75 (2015).
- ²⁰E. H. Putley, *J. Phys. C* **8**, 1837 (1975).
- ²¹See supplementary material at <http://dx.doi.org/10.1063/1.4905922> for additional details and plots (Figure S1-S4) regarding the $A = 1$ and $A = 5$ calculations as well as the effect of a varying mass ratio on the charge neutrality equation.
- ²²O. Madelung, *Semiconductors: Data Handbook* (Springer-Verlag, Berlin, 2004).
- ²³G. S. Nolas, J. Sharp, and H. J. Goldsmid, *Thermoelectrics: Basic Principles and New Materials Developments* (Springer-Verlag, Berlin, 2001).
- ²⁴D. Mandrus, A. Migliori, T. W. Darling, M. F. Hundley, E. J. Peterson, and J. D. Thompson, *Phys. Rev. B* **52**, 4926–4931 (1995).
- ²⁵H. Hohl, A. P. Ramirez, C. Goldmann, G. Ernst, B. Wolfing, and E. Bucher, *J. Phys.: Condens. Matter* **11**, 1697 (1999).
- ²⁶Q. Shen, L. Chen, T. Goto, T. Hirai, J. Yang, G. P. Meisner, and C. Uher, *Appl. Phys. Lett.* **79**, 4165–4167 (2001).
- ²⁷A. D. LaLonde, Y. Pei, H. Wang, and G. J. Snyder, *Mater. Today* **14**, 526–532 (2011).
- ²⁸W. Liu, K. C. Lukas, K. McEnaney, S. Lee, Q. Zhang, C. P. Opeil, G. Chen, and Z. Ren, *Energy Environ. Sci.* **6**, 552–560 (2013).
- ²⁹L. D. Zhao, H. J. Wu, S. Q. Hao, C. I. Wu, X. Y. Zhou, K. Biswas, J. Q. He, T. P. Hogan, C. Uher, C. Wolverton, V. P. Dravid, and M. G. Kanatzidis, *Energy Environ. Sci.* **6**, 3346–3355 (2013).
- ³⁰B. Poudel, Q. Hao, Y. Ma, Y. Lan, A. Minnich, B. Yu, X. Yan, D. Wang, A. Muto, D. Vashaee, X. Chen, J. Liu, M. S. Dresselhaus, G. Chen, and Z. Ren, *Science* **320**, 634–638 (2008).
- ³¹A. J. Minnich, M. S. Dresselhaus, Z. F. Ren, and G. Chen, *Energy Environ. Sci.* **2**, 466–479 (2009).
- ³²F. Yu, J. Zhang, D. Yu, J. He, Z. Liu, B. Xu, and Y. Tian, *J. Appl. Phys.* **105**, 094303 (2009).
- ³³J.-H. Bahk and A. Shakouri, *Appl. Phys. Lett.* **105**, 052106 (2014).